Vibration health monitoring for tensegrity structures

Nasseradeen Ashwear*, Anders Eriksson

KTH Mechanics, Royal Institute of Technology
Osquars backe 18, SE-100 44 Stockholm, Sweden

Abstract

Tensegrities are assembly structures, getting their equilibrium from the integrity between tension in cables and compression in bars. During their service life, slacking in their cables and nearness to buckling in their bars need to be monitored to avoid a sudden collapse. This paper discusses how to design the tensegrities to make them feasible for vibrational health monitoring methods. Four topics are discussed; suitable finite elements formulation, pre-measurements analysis to find the locations of excitation and sensors for the interesting modes, the effects from some environmental conditions, and the pre-understanding of the effects from different slacking scenarios.

Keywords: Tensegrity structure, Vibration Health monitoring, frequency response function, dynamic stiffness, pre-simulations

1. Introduction

When a set of bars and cables are connected by pin-joints, such that the unilateral (all the cables in tension and all bars in compression) properties

*Corresponding author. Tel +4687906184
Email address: ashwear@mech.kth.se (Nasseradeen Ashwear)

are satisfied, the assembly is called a tensegrity structure [1]. Tensegrities are self-stressed pin-jointed structures [2]. [3] classified tensegrity structures as "class k", with k being the maximum number of bars that are connected to each other at any joint. Their stiffness and self-equilibrium rely on the level of pre-stress. Thus, any change in any component status (tension in the cables or compression in the bars) will be reflected in the levels of pre-stress in all components of the whole structure. Therefore, the natural frequencies of the structure are functions of the level of pre-stress [4–7]. In the design of large and complex structures, a Form-Finding methods is commonly adapted [8–10]. The Form-Finding step will normally produce a unit vector $\hat{\boldsymbol{g}}$, containing a set of the force density (N_i/L_s^i) in each component i, with L_s^i the pre-defined final length of each component and N_i the axial internal force. This vector, which is a null-vector of the equilibrium matrix, shows the proportions of component pre-stress forces which will give an externally un-loaded equilibrium state of the structure. The unit self-stress vector $\hat{\boldsymbol{g}}$ is then scaled by a scalar ψ representing the level of pre-stress to give the self-stress vector $\boldsymbol{g}$, with components $g_i = \psi \hat{g}_i$.

Vibration health monitoring (VHM) methods use the modal parameters, such as natural frequencies and mode shapes, as damage-sensitive features [11]. These methods, although differently applied, can also be used as indicators for the design requirement satisfaction, and therefore as quality control tools [12]. A review and more details about the VHM methods can be found in [13].

In the literature, the number of publications about real applications of vibration health monitoring on tensegrity structures is very low. [14] experimentally applied the VHM method as a damage detection tool for a single module tensegrity structure, and for a tensegrity grid structure. The preplanning for the application of the VHM is not reported.

The aim of this paper is to emphasize some topics and issues that might affect the application of VHM on a tensegrity structure, and to suggest a solution for each discussed issue. The paper starts by defining and discussing the more accurate finite elements that must be used in simulations of tensegrity structures for VHM application purposes. Using the results from finite element analysis (FEA), we discuss planning methods for finding the best locations for exciters and sensors, assuming that it is preferred to keep the excitation point fixed for all modes in the range of interest. In addition, effects from the environmental conditions have been considered, with the environmental temperature as an example. Finally, the need for deep understanding of the effects from different slacking scenarios is emphasized. A full creation of an VHM algorithm is not the aim of this paper, but general guidelines are suggested for the application of VHM to tensegrity structures, and with relevance also to other cable and network structures. We thereby consider the design stage, and how pre-simulations at this stage can make VHM measurements possible and useful. Essentially, the pre-simulations will be able to answer two questions: what are the correct dynamic properties of the structure, and how can practical measurements best be performed?

2. Finite element formulation

The internal force in each component of a tensegrity structures is generally assumed to act only in the axial direction of the component. The axial forces in the components are initially introduced by a pre-stressing of the components at manufacturing, but they will be continuously adapting as a function of the external forces on the structure. A tensile axial force in a component will increase its transversal stiffness, which subsequently gives effects on vibration properties in the same way as the tuning of a string in a musical instrument. This effect will then be reduced from a slacking of the cable due to damage. Increasing the compressive internal forces in any bar will on the other hand decrease its transversal stiffness as an effect of nearness of buckling. Slacking cables or bars near to buckling will typically reveal themselves by reduced stiffness and increased tendency to transversal vibrations, and lower natural frequencies. Thus, the finite elements used in simulations must have the capability to capture both axial and transversal vibration in order to give the full dynamic response properties at a particular state. In previous work, we have used Euler-Bernoulli beam elements, in which one-way coupling is introduced to include the effect of the axial force on the transversal stiffness, [7, 15]. This addition will allow the representation of not only vibration modes resulting from axial component vibration, but also bending-type modes

The geometric nonlinearity in tensegrity structures must also be considered. This nonlinearity, however, is emphasized by the coupling between the

axial and bending stiffnesses of the component. This effect has been included in the internal forces and the tangent stiffness matrix. As the aim here is to design for VHM purposes, simulations must be able to capture all these mentioned characteristics. The development of the finite element formulation will not be further discussed here, but can be found in [7, 9, 15].

The element-based simulations are here assumed to be used during the design stage of the tensegrity structure. Primarily, they are used in the design of the pre-stress pattern and level, aiming at, e.g., optimal stiffness or a resonance frequency separation for the unloaded structure. They will also show the response to relevant external loading situations. An important aspect during the design stage is the possibility to evaluate a dynamic signature for the structure, showing the vibration properties which should be shown by the structure if assembled and pre-stressed according to the design. These properties are then preferably evaluated for an externally un-loaded state, as the external loadings will change the forces in the components, and thereby the vibration properties.

3. Pre-measurement analysis

One of the main factors affecting the possibilities to use VHM is the inaccuracy in results from measurements. The pre-measurement analysis must be considered in the design stage of the tensegrity structure along with other design parameters and requirements. It is noted that this demands that the simulation model is detailed and accurate enough for the results to be well

predicting reality.

Normally, the pre-measurement analysis includes two important topics, namely the selection of excitation and sensor points. From a practical point of view, one can change the excitation point easily, but it is from several viewpoints preferred to keep this fixed during a measurement campaign. This assumption is made in the discussion below. The objective is thus to find one excitation point, which can give clear differences in responses for a chosen set of sensor points over an interesting excitation frequency range.

In addition to the response and excitation point selection, the range of interesting frequencies must also be pre-decided. In VHM, normally the lowest natural frequency is utilized [16], but some higher modes might provide further information regarding damage detection and localization. In this paper, we assume that only two of the lowest natural frequencies are of interest, but the same line of thinking can be applied to more extensive ranges.

There are many suggestions in literature with the objective to find methods to evaluate where to excite the structure, and where to install the sensors in order to capture the interesting modes accurately and efficiently. Some of these methods deal with the response locations (sensor placement) only, whereas other methods are developed to find both best excitation and sensor locations. For sensor placement, methods based on kinetic energy, effective independents or eigenvector products can be used. For finding the excitation point, methods based on point residues, kinetic energy or eigenvector products can be used. A summary of these methods and the corresponding

developed techniques can be found in [17] and a comparison can be found in [18].

Recently, many researchers developed methods for placement of sensors and locating the excitation points through optimization methods [19, 20]. Some real measurements of vibrations of tensegrity structures have been done and results published [21, 22]. These, however, do not exclusively discuss the possibilities with pre-measurement analysis, which might reduce the variations between real and numerical results if the pre-simulations are accurate enough. A connection between pre-simulations and vibration measurements would be an important step in the further development of VHM methods for tensegrity structures.

Suitable methods and demands for pre-measurement analysis may well depend on the aim of the measurements. For instance, system identification, where an initially unknown structure is investigated for its dynamic properties, requires more measurement points than VHM, where only a few of the first lowest natural frequencies are normally utilized. The focus was here only on two of the lowest natural frequencies, assuming that these will be used in an VHM strategy. However, the main purpose here was not to develop a new technique for locating the excitation and sensor points, but only to give advices for integrating VHM perspectives during the design stage of the tensegrity structure. In this study, the locations for excitation and sensor points was found manually, but an automatic algorithm can be developed for this purpose, even if a universally valid procedure is not obvious. A brief

explanation of related terms used is first given.

Modal analysis and frequency response analysis are the main parts of the pre-measurement analysis. Modal analysis is defined as the process of finding the natural frequencies, damping factors (if this is considered) and the mode shapes of the system under consideration. It is noted that this evaluation takes place during the design stage, and therefore for the ideal structure as modelled. These are the dynamic characteristics of the structure and are determined completely by its spatially distributed physical properties; mass, stiffness and damping. The modal analysis in the pre-simulations is thereby clearly separated from modal testing, which is an experimental technique used to determine the natural frequencies and the damping factors in their modal forms on the physical structure.

The frequency response analysis of the structure is concerned with finding the response of the structure, normally expressed in a matrix form known as a frequency response function matrix (FRF), below denoted $\boldsymbol{R} = \{R_{ij}\}$ which is frequency dependent $\boldsymbol{R} = \boldsymbol{R}(\omega)$. The notation $\boldsymbol{R}$ is here used as a general response matrix, for any class of quantities. Each element of the this matrix hereby represents the response, which can be displacement, the velocity or the acceleration or their inverses, of the structure in the i^{th} degree of freedom due to a harmonic input of a certain excitation frequency in the j^{th} degree of freedom [23]. It will below be specialized to express the displacement response values in the dynamic flexibility matrix, which is commonly the most easily measured quantity.

The discussion here is based on generating $\boldsymbol{R}(\omega)$ of the tensegrity structure based on its mass $\boldsymbol{M}$ and tangent stiffness matrices $\boldsymbol{K}_T$, evaluated at equilibrium as explained in [7], where it is noted that the vibrations will be seen as linearized around a specified equilibrium configuration. This can be the unstressed or an externally loaded situation, but here primarily the prestressed but otherwise unloaded state is considered.

The procedures for generating the FRFs differ depending on what are the quantities desired. Generation of the dynamic stiffness matrix is required when the direct FRF analysis is adapted. If, on the other hand, the modal FRF analysis is adapted, this will include the solution of the eigenvalue problem to find a few of the normal modes of vibration. Although the latter has lower computational cost, the direct frequency response analysis has been adopted in this study, as this allows the inspection of an FRF matrix to find the suitable excitation point for all interesting modes, and also their suitable measuring points. A modal analysis is however, used to find the signature properties of the structure as designed, and thereby the interesting frequency range of the VHM measurements.

3.1. The frequency response functions FRF

The frequency response functions $\boldsymbol{R}(\omega)$ can be formulated starting from the equations of motion of the structure. When damping is ignored, the equations of motion in matrix form can be simply written as:

$$\boldsymbol{M}\ddot{\boldsymbol{x}}(t) + \boldsymbol{K}_T\boldsymbol{x}(t) = \boldsymbol{f}(t), \tag{1}$$

where $\boldsymbol{M}$ and $\boldsymbol{K_T}$ are the mass and tangent stiffness matrices evaluated at nonlinear equilibrium for the chosen discretized model. The displacements in the model are represented by the vector $\boldsymbol{x}$, and the superposed dot is a time derivative. The equilibrium is typically achieved iteratively using the Newton-Raphson method for the residual force equation [24]. For an assumed harmonic excitation force, the force vector can be expressed as $\boldsymbol{f}(t) = \boldsymbol{F}\sin(\omega t)$, where $\boldsymbol{F}$ describes the spatial distribution of external forces. The displacement vector for the harmonic motion can then be expressed as $\boldsymbol{x}(t) = \boldsymbol{X}\sin(\omega t)$. The dynamic stiffness relation at a particular frequency ω is thereby seen as:

$$(\boldsymbol{K}_T - \omega^2 \boldsymbol{M})\boldsymbol{X} = \boldsymbol{F}, \tag{2}$$

where $(\boldsymbol{K}_T - \omega^2 \boldsymbol{M})$ is the dynamic stiffness matrix, and is a function of the excitation frequency ω. The frequency response matrix for displacements, or the dynamic flexibility matrix, is the inverse of the dynamic stiffness, with necessary boundary conditions introduced, cf. the discussion below. In general, a response function is defined as the ratio between an output and the input, typically as a magnification factor when a particular component is considered, but here absolute vibration amplitudes are considered. In terms of the displacement as an output, the dynamic flexibility matrix $\boldsymbol{H}(\omega)$ can be expressed as an FRF according to:

$$\boldsymbol{H}(\omega) = (\boldsymbol{K}_T - \omega^2 \boldsymbol{M})^{-1} \tag{3}$$

This is seen as a description of measurable displacements as functions of an induced excitation, where the rows of the matrix $\boldsymbol{H}$ are corresponding to the sensor locations, and its column are related to the excitation locations [23]. It is here implicitly assumed that both excitation and sensing uses positions and directions corresponding to a degree of freedom of the discrete model, and that the excitation can be swept over an interesting frequency range. The matrices $\boldsymbol{K}_T$ and $\boldsymbol{M}$ used in Eq. (3), are the retained matrices after the relevant boundary conditions have been applied.

3.2. Sensor and excitation locations

To ensure that each mode of interest will be well excited and hence well measured, a pre-measurements planning is required to decide the locations of excitation and sensors points. The pre-determined locations of exciters and sensors will minimize the test uncertainty and the best results can be achieved, for either system identification or VHM purposes. The issues of where to install the sensors and where to excite the structure has been studied by many researchers, but the answers are strongly dependent on problem class.

Comparing with the kinetic energy method [25] where it is assumed that the excitation point can be changed, i.e., each mode of vibration will be excited and measured from specifically chosen positions, our aim here is to

use one excitation point for the modes of interest and specific sensor point for each mode. The objective is thus not to find the absolute maximum ratio between response and excitation amplitudes for a specific frequency, but to find an excitation point, which will give high but also discriminating response amplitudes in a set of points over a chosen frequency range. An example will show the ambitions.

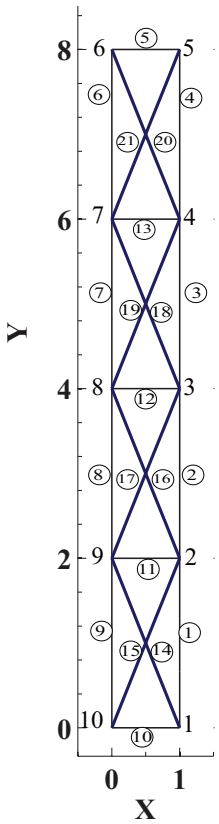

Fig. 1 Four-module X-frame tensegrity structure, with topology, coordinates and the numbering scheme.

3.3. Example

An example is given by the 2D tensegrity structure in Fig. 1, which is composed of four X-frame modules, with a designed size of 1×2 m^2 for each module, and a target structure of designed size 1×8 m^2. Massive circular bars and cables were used with diameters of 0.05 m and 0.015 m for compressed and tensioned components, respectively. For support conditions, node number 1 was fixed in the X and Y directions, and node number 10 in the Y direction. The structure was modelled with beam element, [7, 9], and used four elements for both compressed and tensioned members, giving a total number of 251 degrees of freedom. Hinged joints were modelled by using one rotational degree of freedom for each member attached to the joint.

The values of the unit self-stress vector $\hat{\boldsymbol{g}}$ used is shown in Table 1 and the level of pre-stress applied was $\psi = 18.23$ kN. With this, the first two natural frequencies of the structure are separated [9]. More details about finding the unit self-stress vector $\hat{\boldsymbol{g}}$ for the whole structure can be found in the reference.

The effect of the pre-stress on the first natural frequency of a tensegrity structure can be very low depending on the design, and can even vanish in a certain range of pre-stress [6, 26]. This is the case of the 2D example considered here, where its first natural frequency is approximately unaffected by the level of pre-stress. The frequencies ω_2 and ω_3 are well separated using the optimum design parameters from [9]. The resonance frequencies for this design were first evaluated as $\omega_2 = 116.80$ s^{-1} (18.59 Hz), and $\omega_3 = 120.66$ s^{-1}

Table 1 Force density coefficients of the four module structure in Fig. 1

Component #	(g_i)	Component #	(g_i)
1,9	0.228	13	0.203
2,8	0.225	5	0.100
3,7	0.206	14,15	-0.225
4,6	0.201	16,17	-0.252
10	0.114	18,19	-0.230
11	0.226	20,21	-0.224
12	0.216		

(19.21 Hz), where it is noted that the first resonance frequency $\omega_1 = 37.06$ s^{-1} (5.89 Hz) is almost un-affected by any parameter for this design.

As a practical request, the primary objective has been to find a location where both the second and third modes can be excited from the same point, but with as far as possible different frequency dependencies in response. For a problem of limited size, this can be done by inspection, but it is obvious that within the present problem class the results can be obtained algorithmically. With the aim to keep the excitation point fixed, this was visually chosen in the matrix $\boldsymbol{H}(\omega)$ over the range $17.825 \leq \omega \leq 19.226$ to be at degree of freedom 231, corresponding to the X component of the mid point of bar number 20, Fig. 1.

Examples of unwanted locations are the ones represented by the matrix component, whose frequency dependent displacement amplitudes are $h_{(102,231)}$ and $h_{(150,231)}$ shown in Fig. 2. The first senor location is thereby the degree of freedom 102 corresponding to the X component of node 9, Fig. 1. The other sensor located at the degree of freedom 150 corresponding to

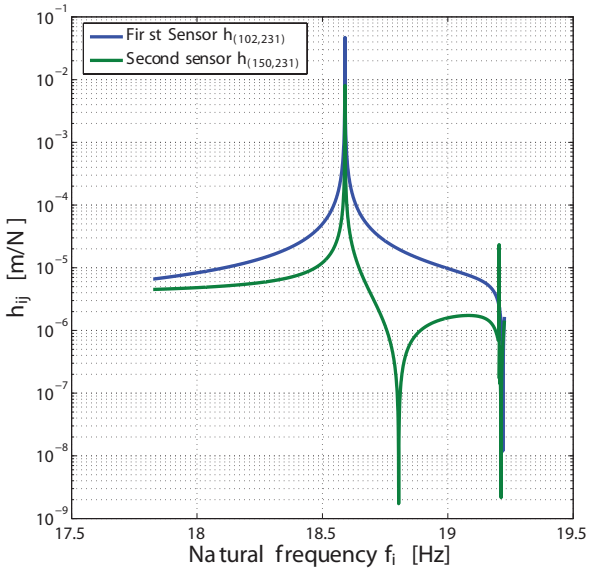

Fig. 2 Displacement amplitudes at two sensor points.

the X component of a point located on cable number 13 and close to node 4, Fig. 1. In this setup, amplitudes responses were clear, but the second sensor detected both the first and second mode from the same location of excitation.

A preferred setup is when the two modes give maximum (or close to maximum) amplitudes at different places. In the flexibility matrix, a visual inspection of the variations with frequency investigated different degrees of freedom (rows) for the sensor. Results showed that it is possible, at least for this simple example, to find a single excitation point and two different sensor locations, as shown in Fig. 3. The diagram was produced by sweeping the excitation frequency over the chosen range of interesting frequencies, and recording the value of h_{ij} from the matrix $\boldsymbol{H}(\omega)$. It is here important

to avoid evaluating the undamped dynamic stiffness matrix exactly at the pre-simulated resonance points when sweeping the frequencies of excitation. The optimal pre-measurement plan is shown by Fig. 3 where the two sensors detected one mode of vibration each for the same excitation point. The first sensor place was kept at degree of freedom 102 while the other sensor location has changed to the degree of freedom 143, the Y direction of a point at the middle of cable number 12.

4. Consideration of environmental effects

Vibration health monitoring methods are based on the change in one or more vibration properties of the structure. In general, it is mostly assumed that the change is caused by damage. Environmental conditions such as wind, snow and temperature changes can cause an equivalent change to the vibration properties as those produced by damage [27] or under operational loads [28]. Effects from snow and wind are not considered in this paper, and to the author's knowledge they are not frequently dealt with in literature. Thus, the focus here was on the temperature effects, as this is the most common source of confusion in any vibration health monitoring algorithm [29–32]. A previous study [15], investigated by simulations the effects from the environmental temperature changes on the natural frequencies of tensegrity structures, and concluded that these can be greater than the effects caused by slacking in one of the cables. It was further shown that these effects are highly dependent on material, support conditions, size and shape

of the tensegrity structure and the level of pre-stress.

Two solutions were proposed in [33] to avoid the effects from the envi-

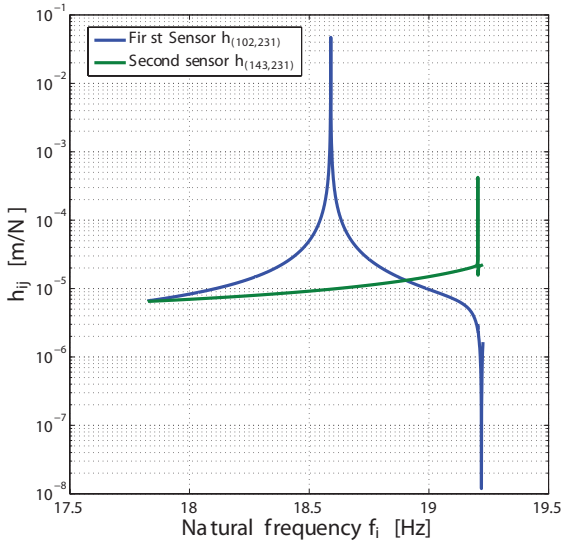

Fig. 3 Displacement amplitudes at two sensor points.

ronmental changes on the natural frequencies. The development was aimed to distinguish the changes originating in damage and the ones from temperature changes. It is also shown that it is possible to design the structure such that some of its lowest natural frequencies are not overly sensitive to temperature changes.

The effects from temperature changes on the natural frequencies of tensegrity structures have two origins. First, they can be related to the changes in the elastic modulus with temperature [34, 35]. They can secondly be related to a temperature dependent in the thermal expansion coefficient [15]. These two effects are thereby related to the materials used, a choice, which is also affected by the optimal design chosen. A conclusion from the work is

that different materials, with different temperature dependencies, might be an optimal choice in a particular structure.

In practice, most materials have a positive thermal expansion and are expanding with increasing temperatures, even if there are some materials like zylon which behave in the opposite direction. These materials are normally too expensive for general earth-bound structures, and the discussion is here limited to the materials that have a positive constant. Assuming that the temperature changes are not localized, changing the length of bars and cables by temperature action occurs synchronously. These changes also affect the pre-stress level such that increasing the unstressed lengths of bars will increase the level of pre-stress while increasing the lengths of cables will decrease it. The response of a general structure to synchronous temperature change can effectively be seen as "cable-dominated" or "bar dominated"describing the overall structural frequency response to pre-stress level.

In the Form-Finding for the tensegrity structures described above, the pre-stress is described by a unit vector $\hat{\boldsymbol{g}}$ representing a self-stress state and a pre-stress level ψ. These gives a pre-stress force $g_i = \psi \hat{g}_i$ in each component. The axial internal force can be also calculated as $N_i = EA_i[L_i^s - L_i(T_o)]/L_i(T_o)$ with E the elastic modulus and A_i the unstressed sectional area. Form this, the unstrained length L_i at the design temperature T_o can be calculated as:

$$L_i(T_o) = EA_iL_i^s/(N_i(\psi) + EA_i), \tag{4}$$

The unstrained length at any temperature T will thereby be:

$$L_i(T) = L_i(T_o)[1 + \alpha\Delta T], \tag{5}$$

where $\Delta T = T - T_o$ and α is the expansion coefficient measured in $1/^{\circ}$C. The modulus E in Eq. (4) is the elastic modulus as a function of temperature. This variation was given for steel materials by [35] as:

$$E(T) = E_{20}(-0.000835T + 1.0167), \tag{6}$$

where E_{20} is the elastic modulus at 20°C, and T should be introduced in °C.

As mentioned above, temperature effects will change the level of pre-stress and hence, the natural frequencies. By substituting Eqs. (4) and (6) into Eq. (5), the unstrained lengths can be found as a function in the environmental temperature T and the level of pre-stress ψ. The whole problem setting and a finite element formulation can be found in [7, 9, 15].

As mentioned above, one solution to the temperature dependence problem is based on the regulation of the pre-stress level or on choosing a proper pre-stress vector. The problem was in [33] seen as an optimization problem, where the level of pre-stress gave the optimization variables, and the change in the natural frequency was the objective to minimize. In order to regulate the level of pre-stress, a Genetic Algorithm (GA) [36], from the built-in functions of

Matlab[1] was used to solve the optimization problem. For the sake of brevity, only the second solution is explained here, the full investigation and a more complex example can be found in [33]. The solutions can be summarized as:

- Using a uniform self-stress vector, where the level of pre-stress is regulated such that the natural frequencies are not affected by temperature changes.

- Using an non-uniform self-stress vector, where the pre-stress in each module is regulated until the natural frequencies of the structure become approximately non-affected from temperature change.

4.1. Example

The structure shown in Fig. 4, with four cables and one bar, is getting its stability from the integrity between tension in the cables and compression in the bar. The four cables were assumed as massive with a diameter of 0.015 m and the bar with 0.1 m. The unstrained lengths $L_i(T_o)$ for all components, were assumed to be cut at T_o=20°C.

The example used $\rho = 7585$ kg/m^3, $\alpha_c = 9 \times 10^{-6}$/°C and $E_{20} = 190$ GPa for cables, and $\rho = 7585$ kg/m^3, $\alpha_b = 11.5 \times 10^{-6}$/°C and $E_{20} = 210$ GPa, for the bar. Nodal coordinates are shown in Table 2. The unit self-stress vector used was $\hat{\boldsymbol{g}}$ =[0.299 0.299 0.299 0.299 -0.889]^T with the final value for the bar. An example for non optimal solution is when the level of pre-stress of $\psi = 21$

[1]Version 2013a, the MathWorks, Inc., Natick, U.S.A.

kN/m is applied, where the first natural frequency is affected by temperature changes Fig. 5 (a). Figure 5 (b) shows the results for the optimal design case when $\psi = 27.24$ kN/m, for which the first and second natural frequencies only marginally change with temperature.

With non-optimal design ($\psi = 21$ kN/m), and at $\Delta T = 0$ °C, the first

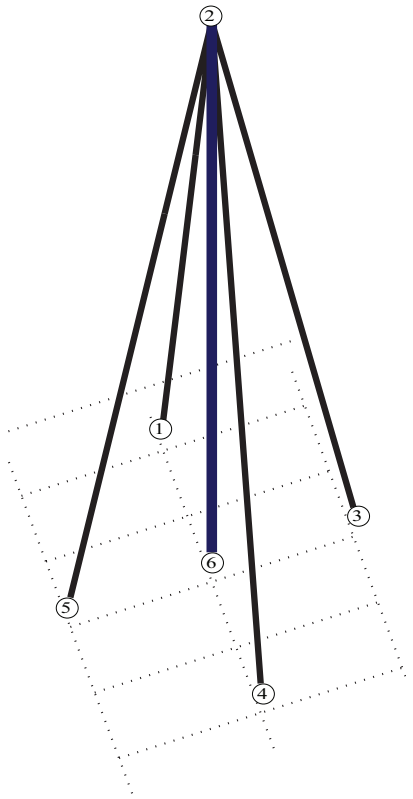

Fig. 4 Four cables and one bar structure.

natural frequency $\omega_0^1 = 16.76$ Hz, while for $\Delta T = -40$ °C, $\omega_{-40}^1 = 16.18$ Hz. The same change from ω_0^1 to ω_{-40}^1 can be made by relaxing one of the cable's unstrained lengths from $L = 3.160$ to $L = 3.161$. It is worth mentioning that the change in the first natural frequency is depending on many other fac-

tors, such as whether the structure is cable or bar dominated, the geometry and material used and, primarily the level of pre-stress [15]. From the VHM viewpoint, the similarity between the change in the first natural frequency, made by temperature changes and by the reduction in the tension in one of the cables, is a cause of uncertainty.

When considering the optimum design of the same structure ($\psi = 27.24$ kN/m), the first natural frequency at $\Delta T = 0$ °C is $\omega_0^1 = 18.17$ Hz. A temperature decrease of $\Delta T = -40$ °C gives $\omega_{-40}^1 = 18.13$ Hz. On the other hand, an increase of temperature of $\Delta T = 20$ °C give $\omega_{26}^1 = 18.11$ Hz. Because both increasing and decreasing the temperature has almost no effect on the first natural frequency, any change in the first natural frequency is certainly caused by a presence of damage.

This example indicates that, for better VHM reliability, the level of pre-stress in the tensegrity structure can be optimized during design to ensure that a set of the lowest natural frequencies are not overly sensitive to environmental temperature changes, thereby improving the possibilities to detect damage to the structure.

5. Effects from different slacking scenarios

The pre-stress pattern and level are important parameters affecting the stiffness and stability of tensegrity structures. However, the pre-stress situation can be altered by many different factors, such as environmental factors like temperature changes. These must be considered when performing vibra-

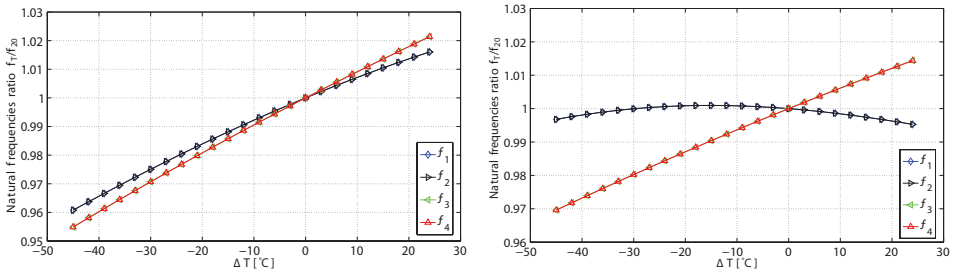

(a) Non-optimal, $\psi = 21$ kN/m (b) Optimal, $\psi = 27.24$ kN/m

Fig. 5 The change of the lowest natural frequencies of the structure shown in Fig. 4.

Table 2 Nodal coordinates of the tensegrity structure shown in Fig. 4.

	Coordinates [m]		
Node No.	X	Y	Z
1	2.0	3.0	0.0
2	2.0	2.0	3.0
3	1.0	2.0	0.0
4	2.0	1.0	0.0
5	3.0	2.0	0.0
6	2.0	2.0	0.0

tion measurements. The most common cause of the degradation of the level of pre-stress is the slacking in the cables caused by a damage at one of the joints. These are one of the primary effects which an VHM measurements is directed towards finding.

Two important points need be emphasised in this context. One is related to damage detection, indicating that some differences exist in relation to the designed situation, either immediately after assembly or as a long-term integrity index. The second point is the more complex, as it is related to damage localization, i.e., a usage of the obtained measurement results to in-

dicate where a degradation has occurred. For damage detection, the ability to differentiate between the changes caused by the environmental conditions and the ones caused by damage is required, as was discussed above.

For the damage localization, a deep understanding of the effects from the slacking in each cable or group of cables is very important. If the effect from the slacking in two cables is similar, then the higher modes might provide useful information to differentiate between the two effects in this case. In general, each structure must be studied and understood separately to understand the effects of each slacking scenario for that particular structure on its natural frequencies. Such studies are facilitated by extensive design stage simulations of the structure, evaluating the typical response function spectra for introduced defects in the structure.

5.1. Example

The T-3 one module tensegrity structure shown in Fig. 6 was chosen to express the need for understanding of the effects from different slacking scenarios. It has 3 bars and 9 cables, with 6 nodes and coordinates listed in Table 3. Massive bars and cables were used with diameters of 0.07 m and 0.014 m, respectively. The structure was simulated with support conditions applied such that node 1 is completely fixed, node 2 fixed in Y and Z directions and node 3 fixed in Z direction. The singular value decomposition of the equilibrium matrix shows that the structure has a unique unit self-stress vector $\hat{\boldsymbol{g}}$, and its values are: 0.094 for the top and bottom cables, 0.238 for

the side cables and -0.416 for the bars. The level of pre-stress $\psi = 90$ kN/m was applied.

At the healthy situation, the first natural frequency is $\omega_1 = 1.03$ Hz. To

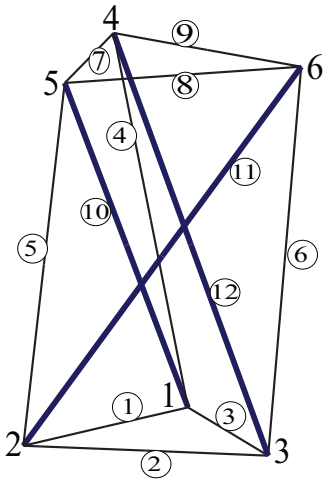

Fig. 6 A T-3 tensegrity structure with its topology and numbering scheme.

show that different slacking scenarios may have different qualitative effects on the first natural frequency, cables 2 and 5 were considered, where a small relaxation in the unstained length of cable 2 from 0.865 m to 0.866 m will increase the first natural frequency to 1.98 Hz, while a small relaxation in the unstrained length of cable 5 from 2.012 m to 2.015 m will decrease the natural frequency to 0.71 Hz. Results for the three scenarios are depicted in Fig. 7, where a comparison between them is more feasible for the first and second natural frequencies. For instance, relaxing in cable 5 has major effect in both first and second natural frequencies, but relaxation in cable 2 has a significant effect only on the first natural frequency. This emphasizes

the need for understanding each scenario individually for the proposes of damage detection and localization. A design-stage simulation of dynamical properties can thereby be a powerful guide for coming VHM planning and measurements.

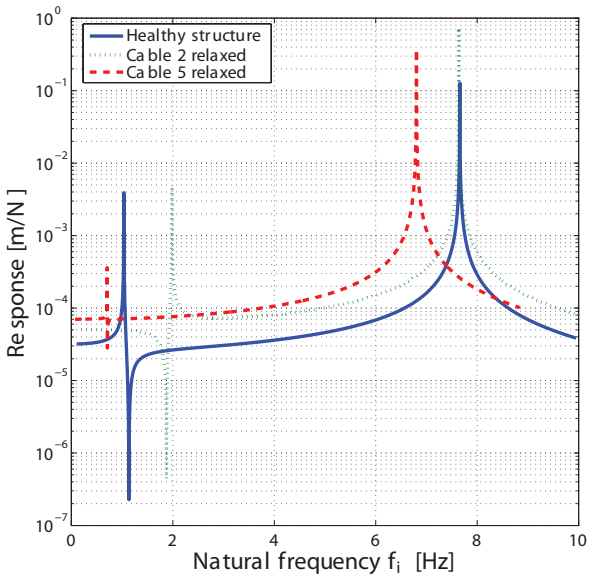

Fig. 7 Natural frequencies of the structure in Fig. 6 indicated from FRF for different cable relaxation scenarios.

	Coordinates [m]		
Node No.	X	Y	Z
1	0.50	0.00	0.00
2	-0.25	0.433	0.00
3	-0.25	-0.433	0.00
4	0.433	0.25	2.00
5	-0.433	0.25	2.00
6	0.00	-0.50	2.00

Table 3 Nodal coordinates of the three-module T-3 tensegrity structure shown in Fig. 6.

6. Summary

Precise measurements are required when implementing any vibration health monitoring method. Hence, a well planned strategy and understanding of the problem is very important. A hypothesis is that simulations of the vibration properties of the structures can and should be performed already at the design stage. These can be used to optimize the design with respect to the VHM demands, but also to simulate the expected effects on the VHM results from degradation, but also from secondary aspects, e.g., variations in environmental parameters. In this paper, we discussed some of the obstacles and suggested some solutions. For the application of vibration health monitoring methods to tensegrity structures, it is important to perform extensive simulations, and in these:

- Choose the right finite element formulations, that can capture both axial and transversal vibrations.
- Do pre-measurement analysis to find the locations for the excitation and the sensors, by generating the frequency response functions—primarily the displacement spectra—based on the dynamic stiffness matrix at the relevant pre-stress and loaded configurations.
- Understand and be able to differentiate between the effects from the environmental conditions and from damage.

- Understand the effects from different slacking scenarios.

References

[1] Fuller R. Synergetics-Explorations in the Geometry of Thinking. Macmillan, London, UK; 1975.

[2] Motro R. Tensegrity: Structural Systems for the Future. Kogan Page Science, London; 2003.

[3] Skelton RE, De Oliveira MC. Tensegrity systems; vol. 1. Springer, London; 2009.

[4] Furuya H. Concept of deployable tensegrity structures in space applications. International Journal of Space Structures 1992;7(2):143–151.

[5] Sultan C, Corless M, Skelton RE. Linear dynamics of tensegrity structures. Engineering Structures 2002;24(6):671–685.

[6] Moussa B, Ben Kahla N, Pons JC. Evolution of natural frequencies in tensegrity systems: a case study. International Journal of Space Structures 2001;16(1):57–73.

[7] Ashwear N, Eriksson A. Natural frequencies describe the pre-stress in tensegrity structures. Computers and Structures 2014;138:162–171.

[8] Tibert AG, Pellegrino S. Deployable tensegrity reflectors for small satellites. Journal of Spacecraft and Rockets 2002;39(5):701–709.

[9] Ashwear N, Tamadapu G, Eriksson A. Optimization of modular tensegrity structures for high stiffness and frequency separation requirements. International Journal of Solids and Structures 2016;80:297–309.

[10] Koohestani K. Automated element grouping and self-stress identification of tensegrities. Engineering Computations 2015;32(6):1643–1660.

[11] Kullaa J. Damage detection of the z24 bridge using control charts. Mechanical Systems and Signal Processing 2003;17(1):163–170.

[12] Salawu O. Detection of structural damage through changes in frequency: a review. Engineering Structures 1997;19(9):718 – 723.

[13] Doebling SW, Farrar CR, Prime MB. A summary review of vibration-based damage identification methods. Shock and Vibration Digest 1998;30(2):91–105.

[14] Panigrahi R, Gupta A, Bhalla S. Damage assessment of tensegrity structures using piezo transducers. ASME Conference Proceedings 2008;.

[15] Ashwear N, Eriksson A. Influence of temperature on the vibration properties of tensegrity structures. International Journal of Mechanical Sciences 2015;99:237–250.

[16] Guechaichia A, Trendafilova I. A simple method for enhanced vibration-based structural health monitoring. Journal of Physics: Conference Series 2011;305(1):012073.

[17] Yuan C, Zhang J. An approach to optimal sensor placement for vibration tests on large structures. In: INTERNOISE 2014 - 43rd International Congress on Noise Control Engineering: Improving the World Through Noise Control. 2014,.

[18] Cinnamon L, David C, Marek L. A comparison of modal test planning techniques: excitation and sensor placement using the NASA 8-bay truss. In: Proceedings of the 12th International Modal Analysis Conference: 1994,Honolulu; vol. 1. 1994, p. 205.

[19] Jung B, Cho J, Jeong W. Sensor placement optimization for structural modal identification of flexible structures using genetic algorithm. Journal of Mechanical Science and Technology 2015;29(7):2775–2783.

[20] Nasr D, Saad G. Sensor placement optimization using ensemble Kalman filter and genetic algorithm. COMPDYN 2015 - 5th ECCOMAS Thematic Conference on Computational Methods in Structural Dynamics and Earthquake Engineering 2015;:3296–3308.

[21] Chan W, Arbelaez D, Bossens F, Skelton R. Active vibration control of a three-stage tensegrity structure. Proceedings of SPIE - The International Society for Optical Engineering 2004;5386:340–346.

[22] Santos F, Rodrigues A, Micheletti A. Design and experimental testing of an adaptive shape-morphing tensegrity structure, with frequency self-

tuning capabilities, using shape-memory alloys. Smart Materials and Structures 2015;24(10).

[23] He J, Fu ZF. Modal Analysis. Butterworth-Heinemann, Oxford; 2001.

[24] Eriksson A. Equilibrium subsets for multi-parametric structural analysis. Computer Methods in Applied Mechanics and Engineering 1997;140(3-4):305–327.

[25] Kammer DC. Sensor placement for on-orbit modal identification and correlation of large space structures. Journal of Guidance, Control, and Dynamics 1991;14(2):251–259.

[26] Ali NBH, Rhode-Barbarigos L, Albi AAP, Smith IF. Design optimization and dynamic analysis of a tensegrity-based footbridge. Engineering Structures 2010;32(11):3650 – 3659.

[27] Farrar CR, Jauregui DA. Comparative study of damage identification algorithms applied to a bridge: I. Experiment. Smart Materials and Structures 1998;7(5):704–719.

[28] Xu YL, Chen B, Ng CL, Wong KY, Chan WY. Monitoring temperature effect on a long suspension bridge. Structural Control and Health Monitoring 2010;17(6):632–653.

[29] Giraldo DF, Dyke SJ, Caicedo JM. Damage detection accommodating varying environmental conditions. Structural Health Monitoring 2006;5(2):155–172.

[30] Xia Y, Hao H, Zanardo G, Deeks A. Long term vibration monitoring of an RC slab: temperature and humidity effect. Engineering Structures 2006;28(3):441–452.

[31] Cornwell P, Farrar CR, Doebling SW, Sohn H. Environmental variability of modal properties. Experimental Techniques 1999;23(6):45–48.

[32] Sohn H. Effects of environmental and operational variability on structural health monitoring. Philosophical Transactions of the Royal Society A: Mathematical, Physical and Engineering Sciences 2007;365(1851):539–560.

[33] Ashwear N, Eriksson A. Reducing effects from environmental temperature on the natural frequencies of tensegrity structures; 2016. Manuscript submitted for possible publication.

[34] Ancas AD, Gorbănescu D. Theoretical models in the study of temperature effect on steel mechanical properties. Bulletin of the Polytechnic Institute of Jassy, Constructions, Architechture Section 2006;LII (LVI)(1-2):49–54.

[35] Kankanamge ND, Mahendran M. Mechanical properties of cold-formed steels at elevated temperatures. Thin-Walled Structures 2011;49(1):26 – 44.

[36] Holland JH. Adaptation in Natural and Artificial Systems. Ann Arbor, MI, USA: University of Michigan Press; 1975.